Molecular engineering versus energy level alignment: Interface formation between oligothiophene derivatives and a metal substrate studied with photoemission spectroscopy

A. J. Mäkinen[a] and I. G. Hill[b]
Optical Sciences Division, Naval Research Laboratory, Washington, DC 20375

M. Kinoshita, T. Noda, and Y. Shirota
Department of Applied Chemistry, Faculty of Engineering, Osaka University, Osaka, Japan

Z. H. Kafafi[c]
Optical Sciences Division, Naval Research Laboratory, Washington, DC 20375

(Received 4 September 2001; accepted for publication 5 February 2002)

Two series of thin films of oligothiophene derivatives grown on Ag substrates have been studied with photoelectron spectroscopy. The oligothiophenes were end-capped with either electron-deficient (dismesitylboryl) or electron-rich (diphenyltolylamine) moieties to create molecules with electron-accepting or -donating properties, respectively. The position of the highest occupied molecular orbital (HOMO) at the metal/organic interface is found to be strongly dependent on the effective π-conjugation length of the oligothiophenes capped with dimesitylboryl groups, whereas in the oligothiophenes capped with diphenyltolylamine, the position of the HOMO is independent of the molecular length. The difference in the observed HOMO characteristics is attributed to the different make-up of the frontier orbitals in the two molecular series. This will particularly affect the overall energy barrier for charge injection at the conductor/organic interface in a device structure, such as an organic light-emitting diode, utilizing the investigated molecules for carrier injection and transport. © *2002 American Institute of Physics.* [DOI: 10.1063/1.1464209]

I. INTRODUCTION

Organic semiconductors have experienced rapid growth in electronic and optoelectronic applications over the past ten years. The device applications of these materials include photoreceptors, batteries, solar cells, field-effect transistors, switches, nonlinear optical components, and organic light-emitting devices (OLEDs), to list a few. Electro- and photoactive organic materials are particularly attractive for application development because of the way in which the design of organic materials can be implemented. Owing to the weak van der Waals bonding between molecules in the solid state, the molecules retain much of their individual character, and therefore the electronic and optical properties of molecular solids can be defined and adjusted *at the molecular level*. A typical device, such as an OLED, consists of a multilayer structure where each layer has a specific function, e.g., carrier injection and transport or charge recombination and light emission. Given the thin-film structure of molecular devices, interfaces between different functional layers have an important role in affecting device operation. In particular, device functions based on charge transport and injection within the layers adjacent to anode and cathode contacts depend critically on the character of the transport levels at and near the film interfaces. Therefore, in addition to the molecular engineering aspects of the active materials for molecular electronics, the interface formation of these materials at the electrodes needs to be considered in device design in order to maximize the efficiency and performance of the device.

In this article, we report an ultraviolet photoemission spectroscopy (UPS) study of interface formation between two series of oligothiophene derivatives and a metal substrate. The oligothiophenes have been functionalized through attaching either electron-deficient or electron-rich end-moieties to the thiophene chain to create either an electron transport or a hole transport material, respectively. More specifically, the first group of oligomers consists of 2,5'-bis(dimesitylboryl)-2,2'-thiophene (BMB-1T), 5,5'-bis(dimesitylboryl)-2,2'-bithiophene (BMB-2T) and 5,5'bis(dimesitylboryl)-2,2':5'2'-tertiophene (BMB-3T), which are characterized as electron transport materials.[1] In the following, this group of oligomers will be referred to as the BMB-nTs where n denotes the number of the central thiophene rings. The second group of molecules for the study consists of 2,5'-bis{4-[bis(4-methylphenyl)-amino]phenyl}-2,2'-thiophene (BMA-1T), 5,5'- bis{4-[bis(4-methylphenyl)amino]phenyl}-2,2'-bithiophene (BMA-2T), 5,5'-bis{4-[bis(4-methylphenyl)amino]phenyl}-2,2'-terthiophene (BMA-3T), 5,5'-bis{4-[bis(4-methylphenyl)-amino]phenyl}-2,2'-quater- thiophene (BMA-4T), which are characterized as hole transport materials.[2] The second group will be referred to as the BMA-nTs. The chemical structures of the BMB-nT and BMA-nT molecules are shown in Fig. 1.

The demonstration of OLED structures utilizing these two series of molecules in their emitting layer has recently been reported.[1–4] The area of focus in these studies has been

[a]Author to whom correspondence should be addressed; electronic mail: ajm@ccs.nrl.navy.mil
[b]Present address: Sarnoff Corporation, Princeton, NJ 08543.
[c]Electronic mail: Kafafi@ccf.nrl.navy.mil

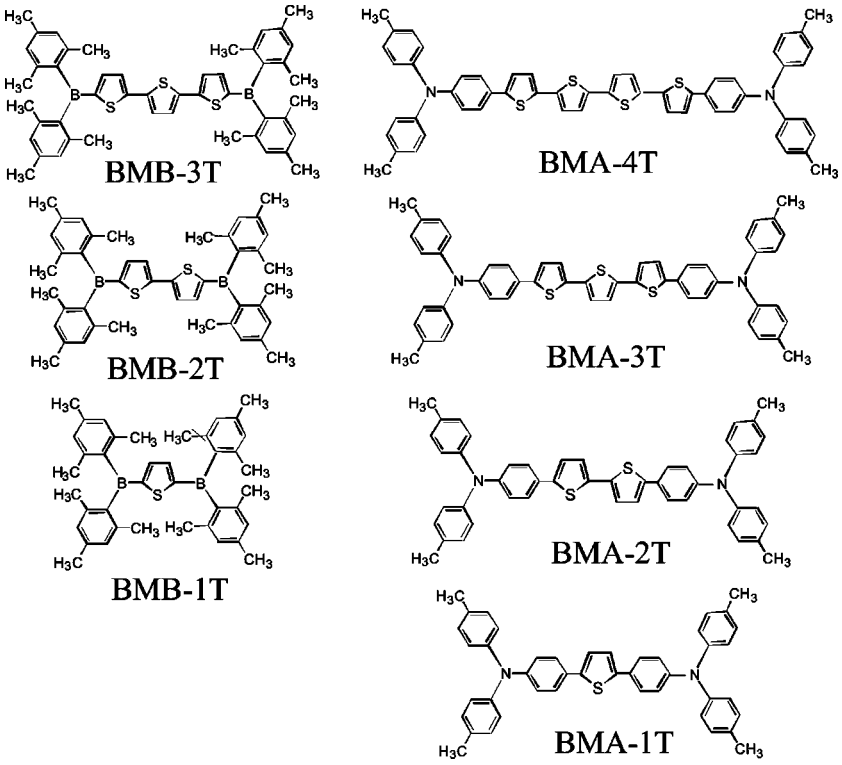

FIG. 1. The chemical structures of the investigated oligothiophene derivatives.

the development of thermally stable electron and hole transport materials with good film-forming properties and color tunability for OLED applications. The film-forming properties of these molecules have been improved by the addition of nonplanar end moieties to the central thiophene rings, which results in the formation of amorphous films upon evaporation. This is in contrast with unsubstituted oligothiophenes that typically form polycrystalline films. The thermal stability of the films of BMB- and BMA-nTs is reflected in their glass transition temperatures which are 71, 107, and 115 °C for BMB-1T, BMB-2T, and BMB-3T, respectively, and 86 °C, 90 °C, 93 °C, 98 °C for BMA-1T, BMA-2T, BMA-3T and BMA-4T, respectively.[4] The fluorescence color tuning is done by controlling the π-conjugation length of the oligothiophene chain. In the BMB-nTs, the most intense emission lines are from deep blue to blue-green: 440 nm (BMB-1T), 440 nm (BMB-2T), 488 nm (BMB-3T) (measured in a tetrahydrofuran solution). The corresponding emission lines of the BMA-nTs are from blue to yellow-green: 456 nm (BMA-1T), 491 nm (BMA-2T), 516 nm (BMA-3T), and 532 nm (BMA-4T) (measured in a tetrahydrofuran solution).[4]

Most recently, we have been able to show that the frontier orbital alignment of BMB-2T and BMB-3T at the metal-organic interface is dependent on the number of thiophene rings present, i.e., the effective π-conjugation length of the molecule.[5] In the current article, we present additional UPS measurements on BMB-1T films grown on an Ag substrate confirming the trend for frontier orbital evolution as a function of the conjugation length in BMB-nTs. We are then able to contrast the behavior of the highest occupied molecular orbitals (HOMOs) of the BMB-nTs at the metal-organic interface with that of the BMA-nTs. In the latter case, the HOMO position at the interface is found to be independent of the molecular length. This is interpreted as the location of the HOMO shifting from the central oligothiophene rings to the end moieties of the BMA-nTs.

II. EXPERIMENT

The ultraviolet and x-ray photoemission spectroscopy (UPS, XPS) measurements were carried out in a two-chamber UHV system (base pressure 10^{-10} Torr) consisting of a preparation and an analysis chamber separated by a gate valve. The organic materials were synthesized and purified as described in detail elsewhere.[2,3] They were placed inside quartz crucibles that were resistively heated to the desired sublimation temperature. Films of the BMA-nT and BMB-nT molecules were vacuum deposited onto a polycrystalline Ag foil, which was first cleaned by ion sputtering. The contamination levels of the Ag substrate were monitored with XPS. The average deposition rate, monitored with a quartz crystal microbalance, was 10 Å/min. After film deposition, the samples were moved from the preparation chamber to the analysis chamber without breaking the vacuum. The film deposition was done layer by layer, and the HeI ($h\upsilon = 21.22$ eV) and HeII ($h\upsilon = 40.82$ eV) spectra were recorded after each deposition using a hemispherical energy analyzer for electron detection. The resolution of the analyzer was set to 50 meV. The sample was biased at -3.0 V to compensate for the contact potential between the sample and the analyzer. Additional XPS core level spectra were measured for selected films using Al $K\alpha$ radiation ($h\upsilon = 1486.6$ eV). The optical absorption spectra of the solid films were measured *ex situ* on a separate set of films evaporated on quartz substrates.

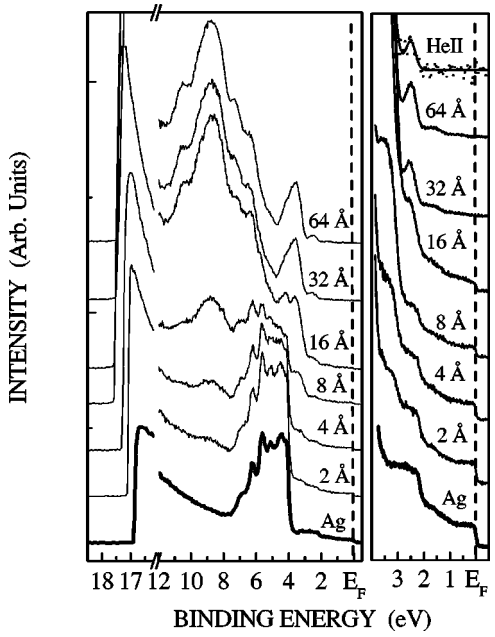

FIG. 2. HeI spectra of BMB-3T films at various thicknesses. The inset shows the HOMO part of the HeI spectra in detail and the HOMO part of the HeII spectrum of a 64 Å-thick film. The binding energy is referenced to the Fermi level (E_F).

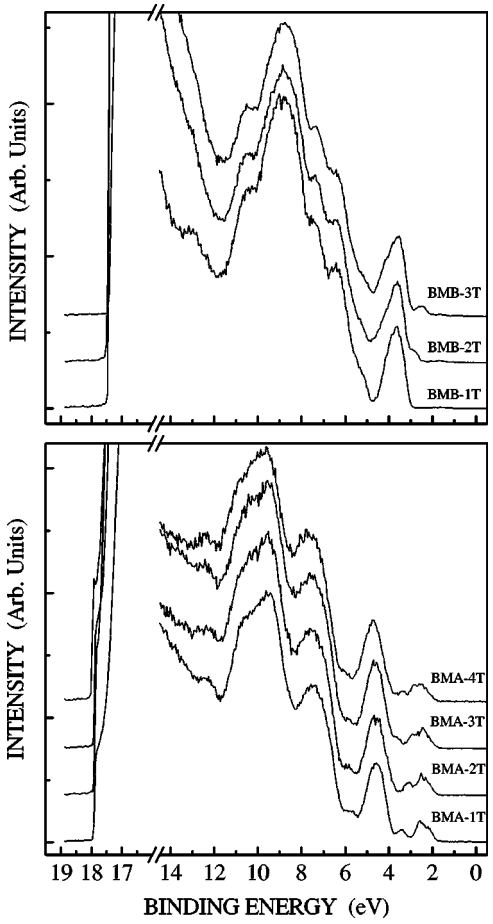

FIG. 3. HeI spectra of 64 Å-thick films of BMB-nTs and BMA-nTs. The binding energy is referenced to the Fermi level.

III. RESULTS AND DISCUSSION

A. Film growth and interface formation

An example of HeI spectra measured for BMB-3T films at different thicknesses is shown in Fig. 2 where the binding energy is referenced to the Fermi level (E_F) of the Ag substrate. As the coverage of the BMB-3T is increased, new features due to the molecular orbitals of BMB-3T quickly appear at the higher binding energies ($\geqslant$8.0 eV) in the HeI spectra. However, the substrate peaks at the intermediate binding energies between 4 and 8 eV remain in the spectra and do not completely disappear until the highest occupied molecular orbitals are fully formed at a nominal coverage of 16 Å. E_F is still visible at this coverage and, given the relatively shallow probing depth of UPS (5 Å), we conclude that the substrate is not fully covered by the molecular film. This may be interpreted as clustering of the molecules at the substrate surface upon evaporation. It also bears noting that the position of the HOMO does not change after 16 Å and with the E_F still visible at this coverage, we can be confident that the energy scale remains the same for the photoemission spectra at higher coverage.

The BMB-3T films show an abrupt shift of the vacuum level at low coverage ($\leqslant$8 Å) after which the level position stays constant with increasing film thickness. This is an indication of a charge dipole layer forming at the metalorganic interface. Since the shift is positive, i.e., there is a shift towards higher binding energies, it implies that the dipole is directed out of the metal surface. Possible mechanisms for the dipole formation include charge transfer between the metal and the organic, chemical reaction, and polarization of the molecular layer due to the image force effect at the interface.[6,7] We find no evidence for charge transfer between the metal and the organic in our spectra, i.e., there are no midgap states or uniform shifts of the peaks observed in the spectra during the initial stages of film growth. XPS measurements on the BMB-3T films grown layer by layer on Ag substrates reveal no evidence for a chemical reaction between the metal and the organic. These findings are in agreement with previous studies which have found no significant chemical reaction between thiophene and a noble metal (Au).[8] Therefore, the most likely mechanism for the dipole layer formation is the polarization of the organic layer at the interface.[9] The features of the film growth and the interface formation discussed in the case of BMB-3T are characteristic of all the BMA-nT and BMB-nT films. These include the general direction of the vacuum level shift and the location of the HOMO, which we shall discuss in greater detail in the following sections.

B. Conjugation length versus orbital structure

1. BMB-nT series

The position of the HOMO level of the BMB-nTs shifts towards lower binding energies with the increasing molecular length as seen in Fig. 3 and in more detail in Fig. 4. The position of the HOMO levels was determined from the edge of the emission cut-off by linear extrapolation. Interestingly, it is only the HOMO levels of the BMB-nTs that are shifted significantly with respect to each other, whereas the spectral features at higher binding energies appear to be very similar

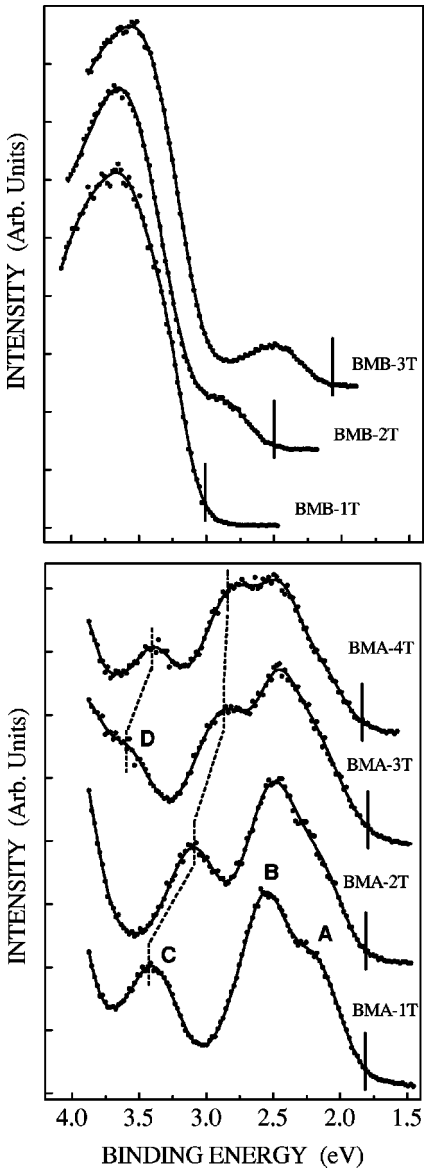

FIG. 4. HeI spectra of the HOMO levels of 64 Å-thick BMA-nT and BMB-nT films. The solid lines indicate a least square fit of a sum of Gaussian functions superimposed on a polynomial background. The solid vertical lines mark the position of the HOMO of each film, and the dashed lines show the movement of the thiophene-related π-orbitals in BMA-nT films. The binding energy is referenced to the Fermi level.

and are located in the same position for all three molecules. The HOMO lines were also observed in the HeII spectra of the films, thus eliminating the possibility that the relatively weak HOMO features of the HeI spectrum might be an artifact of the HeII emission near the minimum binding energy observed in the HeI spectrum.[5] In fact, the HOMO part of the BMB-3T spectra in Fig. 2 has a small feature at 1.5 eV, which is absent in the HeII spectrum. We therefore identify this feature in the HeI spectrum as an artifact due to HeII emission.

The UPS spectra of BMB-1T, BMB-2T, and BMB-3T closely resemble the UPS spectra reported in the literature for bithiophene, terthiophene, and quarterthiophene, respectively.[10,11,12,13] A combination of experimental and computational work has shown that the HOMO levels of unsubstituted oligothiophenes are composed of binding π-orbitals, whose origin can be assigned to the thiophene rings.[12] The interaction between the rings manifests itself as the splitting of the bonding π-orbitals where the number of the split levels is proportional to the number of interacting thiophene rings.[11] Similar level splitting is observed in the low-energy part of the BMB-nT spectra and is reflected in the position of the HOMO and HOMO-1 levels of these molecules. As the number of thiophene rings is increased from one to three in the BMB-nT compounds, the HOMO line initially embedded in a larger feature at 3.6 eV in the BMB-1T spectrum moves towards lower binding energies, becoming clearly separated from HOMO-1 line at 2.5 eV in the case of BMB-3T. Conversely, following the treatments of oligothiophene spectra,[12] we attribute the feature at 3.6 eV, independent of the number of thiophene rings, to the noninteracting orbitals in the repeating units and to contributions from the dimesityl-boryl end-groups.

2. BMA-nT series

In contrast to the trend of the HOMO positions in the BMB-nTs, the HOMO position in the HeI spectra of the BMA-nT films is constant at ~1.8 eV as the number of central thiophene rings (n) increases from one to four. The high binding energy parts of the HeI spectra (>6 eV), on the other hand, appear almost identical—an obvious similarity with the BMB-nTs. A closer look at the spectral evolution near the HOMO energy shown in Fig. 4 reveals a very interesting energy level structure. In the HeI spectrum of BMA-1T, we can identify HOMO, HOMO-1, and HOMO-2 lines located at 2.2, 2.6, and 3.4 eV, respectively (labeled A, B, C in Fig. 4). As the number of thiophene rings increases ($n=1\rightarrow n=4$), peak "C" steadily progresses towards lower binding energies. However, the positions of peaks "A" and "B" are not changed as found from fitting a sum of Gaussian functions superimposed on a polynomial background to the spectra. An additional feature "D" appears at 3.6 eV in the BMA-3T spectrum, shifting to 3.4 eV in the BMA-4T spectrum, which correlates closely with the behavior of peak C.

The explanation for the evolution of the low binding energy levels within the BMA-nT molecules can be found from the chemical structure of the molecules. Since the HOMO and HOMO-1 levels (peaks A and B) are independent of the number of thiophene rings in the BMA-nTs, we attribute the two peaks to the diphenyltolylamine groups at each end of the BMA-nTs. Our assignment of peaks A and B further implies that the frontier orbitals have a considerable contribution from the lone electron pair of the nitrogen atoms, and the phenyl and tolyl moieties. This conclusion is based on experimental results and density functional theory calculations on N,N'-diphyenyl-N,N'-bis(3-methylphenyl)-1,1'-biphenyl-4,4-diamine (TPD),[14,15] which can be viewed as a dimer of diphenyltolylamine. In these studies, it was found that the HOMO of TPD is mostly localized over the biphenyl core and the nitrogen atoms, with some contribution from the side phenyl and tolyl groups.

The shifting of peaks C and D towards lower binding energies with increasing chain length is analogous to the behavior of the HOMO features in the BMB-nT films. In other

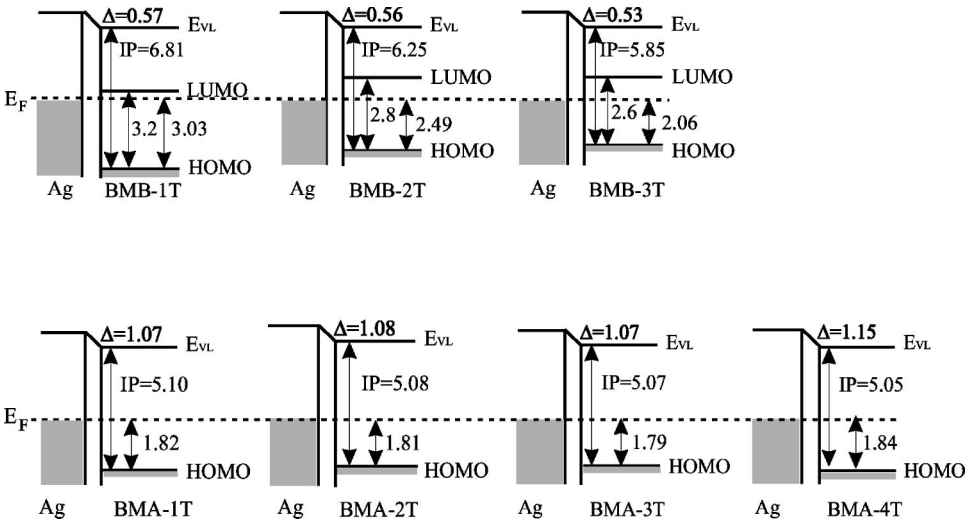

FIG. 5. The energy level alignment at the metal-organic interface. The energy values are expressed in electron volts.

words, the interaction of the bonding π-orbitals in the thiophene units results in the level splitting and shifting observed in the peaks C and D of the BMA-nT spectra. Moreover, the location of peak C in the BMA-3T spectrum is only 0.15 eV lower than the center of the HOMO line of the BMB-3T spectrum when measured from the vacuum level. These two observations indicate that the energy levels of the oligothiophene part in BMA-nT compounds stay largely unperturbed and maintain their spectral characteristics.

3. Molecular planarity and conjugation

It has been found that as the π-conjugation length of the oligothiophene chain is increased beyond 7–8 thiophene rings,[12] the photoemission spectrum of the oligothiophene cannot be distinguished from that of a polythiophene.[11,16] In a UPS spectrum of a polythiophene, the HOMO feature is a band-like distribution of levels originating from a large number of interacting thiophene rings.[11] The difference between the HOMO position of terthiophene and that of polythiophene is approximately 0.5 eV.[12] This yields an estimate for the upper limit of the HOMO of BMB-nT molecules with a longer chain length.

The upper limit for the HOMO position derived from polythiophenes is merely a manifestation of the maximum conjugation length over which the interaction between the π-orbitals of different thiophene units can be perceived. In order for the π-orbitals to interact, the thiophene chain needs to maintain its planarity, which implies an uninterrupted charge conjugation of the chain. The conjugation length therefore appears to have a maximum at 7–8 rings for oligo- and polythiophenes. Hence, the level splitting found in the BMA-nT and BMB-nT spectra indirectly verifies the coplanarity of the thiophene rings, which may be lost should the molecule interact chemically with the substrate.[8]

C. Energy levels at the metal-organic interfaces

The energy level alignment at the metal-organic interfaces is shown in Fig. 5. The ionization potential of a molecular film is equal to the difference between the HeI photon energy and the width of the HeI spectrum. The latter is the difference of the intensity thresholds at the lowest and at the highest binding energies, i.e., vacuum level onset and the HOMO edge, respectively. The band gaps in the BMB-nT films were estimated from the measured optical absorption spectra of the solid films.

Since the vacuum level shifts (Δ in Fig. 5) are practically constant within the BMA-nTs and the BMB-nTs, $\sim$0.55 and $\sim$1.1 eV, respectively, the difference in the ionization potentials is reflected in the positions of the HOMO levels with respect to the Fermi level of the metal. As mentioned earlier, the BMA-nT compounds are characterized as hole transporting materials, and therefore the critical parameter for a device operation is the hole injection barrier at an anode/hole transport layer interface. In a photoemission experiment, the HOMO level marks the highest occupied energy level of a cation with a net positive charge of one, and hence the E_F-HOMO separation is equal to the energy barrier for hole injection from the conductor into the organic. Because of the constant ionization potential of the BMA-nT molecules the hole injection barrier appears to have the same value of $\sim$1.82 eV for each metalorganic interface, and is therefore independent of the π-conjugation length of the BMA-nT molecules.

Assuming similar exciton binding energies (typically 0.2–0.5 eV[17]) in the BMB-nT films, the estimated lowest unoccupied molecular orbits Fermi level separation changes from 0.17 eV in BMB-1T to 0.54 eV in BMB-3T. In other words, the electron injection barrier is expected to increase significantly at the metalorganic interface as the effective π-conjugation length of the BMB-nT molecules gets longer. Here it is useful to point out that in our analysis, we have used the flatband condition to determine the injection levels, i.e., the HOMO position indicated by the flatband in Fig. 5 is determined from the bulk film spectrum (64 Å) and the interface region of the energy levels (where level position is changing), is viewed as a tunneling barrier for charge injection.

The present work was carried out on Ag/BMB-nT and Ag/BMA-nT interfaces, where the Ag foil used in the reported experiments had a work function of 4.32 eV. A real device would typically utilize a metal cathode with a lower work function in order to minimize the electron injection

barrier. Similarly, a high work function metal, e.g., Au, or a conducting oxide, such as indium tin oxide, would be utilized as an anode in order to minimize the hole injection barrier in the device. Although the studied interfaces will not give us the absolute values for typical charge injection barriers, we do expect the observed trend of the energy levels for the two series of oligothiophene derivatives to hold for interfaces in real devices.

Based on the energy level diagrams shown in Fig. 5, the electron injection efficiency is expected to depend strongly on the π-conjugation length of the BMB-nT molecules, whereas the hole injection efficiency will most likely be independent of the molecular length at an anode/BMA-nT interface. From the point of view of molecular and device engineering, it is interesting to see the very different interfacial behavior that results from attaching either an electron-deficient or electron-rich group to the central oligothiophene rings. In a sense, the latter represents almost an ideal case in molecular engineering, namely, the interfacial properties of the BMA-nT molecular films remain the same while the optical and the structural properties can be tailored as a function of the molecular length. This is, of course, assuming that one wants to utilize BMA-nTs both as hole transporters and emitters. The BMB-nTs, on the other hand, present a slightly more complicated case where the interface properties do change along with the chain length. The understanding of how the functionalization of a molecular structure (electron accepting versus electron donating properties) will affect the electronic structure of a metal-organic interface, i.e., the nature and position of the frontier orbitals, developed in this study will be an essential component to be incorporated in materials design.

IV. CONCLUSION

In the photoelectron spectroscopy study of solid films of BMA-nTs and BMB-nTs, we have found that the position of the HOMO levels at the metal-organic interface is strongly dependent on the effective π-conjugation length of the BMB-nTs, whereas in the BMA-nTs, it is independent of the molecular length. We attribute the difference in the observed HOMO characteristics to the different makeup of the frontier orbitals in the two molecular series. In BMB-nTs, the HOMO corresponds to the interacting π-orbitals located on the thiophene rings, while in BMA-nTs, the HOMO is located on the diphenyltolylamine end moieties. This will particularly affect the overall energy barrier for charge injection at an electrode/organic interface in devices and consequently, will greatly influence their performance. Therefore, in addition to tailoring the optical and structural properties of each species to the desired specifications, the interfacial properties resulting from the molecular engineering should also be considered in the design of organic light-emitting diodes or other electro-optic devices utilizing highly fuctionalized molecular structures.

ACKNOWLEDGMENTS

The authors would like to acknowledge the Office of Naval Research for financial support, and Dr. Gary Kushto and Dr. Hideyuki Murata for performing the optical absorption measurements. One of the authors (A.J.M.) acknowledges the NRC for administering the postdoctoral program at NRL.

[1] T. Noda, H. Ogawa, and Y. Shirota, J. Am. Chem. Soc. **120**, 9714 (1998).
[2] T. Noda, H. Ogawa, and Y. Shirota, Adv. Mater. **11**, 283 (1999).
[3] T. Noda, H. Ogawa, N. Noma, and Y. Shirota, J. Mater. Chem. **9**, 2177 (1999).
[4] Y. Shirota, J. Mater. Chem. **10**, 1 (2000).
[5] A. J. Mäkinen, I. G. Hill, T. Noda, Y. Shirota, and Z. H. Kafafi, Appl. Phys. Lett. **78**, 670 (2001).
[6] H. Ishii, K. Sugiyama, E. Ito, and K. Seki, Adv. Mater. **11**, 605 (1999).
[7] H. Ishii and K. Seki, IEEE Trans. Electron Devices **44**, 1295 (1997).
[8] F. Elfeninat, C. Fredriksson, E. Sacher, and A. Selmani, J. Chem. Phys. **102**, 6153 (1995).
[9] I. G. Hill, A. J. Mäkinen, and Z. H. Kafafi, J. Appl. Phys. **88**, 889 (2000).
[10] D. Steinmüller, M. G. Ramsey, and F. P. Netzer, Phys. Rev. B **47**, 13323 (1993).
[11] G. Tourillon and Y. Jugnet, J. Chem. Phys. **89**, 1905 (1988).
[12] H. Fujimoto, U. Nagashima, H. Inokuchi, K. Seki, Y. Cao, H. Nakahara, J. Nakayama, M. Hoshino, and K. Fukuda, J. Chem. Phys. **92**, 4077 (1990).
[13] H. Fujimoto, U. Nagashima, H. Inokuchi, K. Seki, Y. Cao, H. Nakahara, J. Nakayama, M. Hoshino, and K. Fukuda, J. Chem. Phys. **89**, 1198 (1988).
[14] K. Sugiyama, D. Yoshimura, T. Miyamae, T. Miyazaki, H. Ishii, Y. Ouchi, and K. Seki, J. Appl. Phys. **83**, 4928 (1998).
[15] M. Malagoli and J. L. Brédas, Chem. Phys. Lett. **327**, 13 (2000).
[16] C. R. Wu, J. O. Nilsson, O. Inganäs, W. R. Salaneck, J. E. Österholm, and J. L. Bredas, Synth. Met. **21**, 57 (1987).
[17] C. I. Wu, Y. Hirose, H. Sirringhaus, and A. Kahn, Chem. Phys. Lett. **272**, 43 (1997).